

# ADVANTAGES OF USING DPSS NANOSECOND LASER WITH A GAUSSIAN BEAM SHAPE FOR SCRIBING THIN FILM PHOTOVOLTAIC PANELS

Paper #M1101

Ashwini Tamhankar<sup>1</sup>, James Bovatsek<sup>1</sup>, Gonzalo Guadano<sup>2</sup>, Rajesh Patel<sup>1</sup>

<sup>1</sup>Spectra Physics, a division of Newport Corporation, 1330 Terra Bella Ave, Mountain View, CA, 94043, USA

<sup>2</sup>Lasing SA, Marques de Pico Velasco, 64, 28027 Madrid, Spain

## Abstract

Laser scribing of various thin film materials is a key process in manufacturing of thin film photovoltaic (PV) panels. In recent years, PV industry has adopted the use of high-power nanosecond-pulse diode pumped solid state (DPSS) Q-switch lasers to increase precision and throughput of scribe processes. A major push for the use of lasers is made in order to increase the quality of scribes and hence the efficiency of a solar cell while reducing fabrication costs. This paper focuses on identifying advantages of using a Gaussian shaped laser beam from a DPSS Q-switch laser for thin film scribe processes. In particular, scribing with a Gaussian laser beam and a flattop shaped laser beam has been evaluated and compared. From a laser scribing system design perspective, the effect of beam intensity distribution on the process depth of focus has been characterized. In addition, scribing with a high quality low  $M^2$  Gaussian beam from a DPSS q-switch laser and a beam from a high  $M^2$  fiber laser has been compared. Again from a laser scribing design perspective, the effect of each laser on process depth of focus has been characterized.

## Introduction

Laser technology is being widely used in manufacturing of thin film photovoltaic (PV) panels for building solar cells [1]. Lasers are one of the major contributors in reducing manufacturing costs while increasing efficiency of solar cells. A robust integrated system design is necessary to achieve highest quality scribes at a very high yield. Usually to accommodate large solar panel glass variations combined with other system variations there is often a need for accommodating 1 to 3mm depth variation during scribing process. This variation gets worse as the glass panel size increases. Thus a system design that can accommodate higher depth variations and can produce quality scribes is highly desirable from manufacturing perspective. Hence, in this paper we have explored the effects of laser beam shape as well as beam quality on

process depth of focus. The process depth of focus has been defined as distance along the laser beam propagation axis within which an electrically isolated good quality scribes can be achieved by a given laser scribing system.

In recent years, the thin film photovoltaic (TFPV) industry has adopted the use of high-power nanosecond pulse diode pumped solid state (DPSS) Q-switch lasers to increase precision and throughput of thin film solar cells scribe processes [1]. A typical TFPV device consists of three layers deposited onto a glass substrate. The first layer is a conductive material; either a transparent conducting oxide (TCO) such as Zinc Oxide (ZnO), Tin Oxide (SnO<sub>2</sub>) or an opaque metallic material such as Molybdenum (Mo) deposited on glass, the middle layer is the active semiconductor layer and the third layer is another conductor; either TCO, aluminium (Al) or combination of both. These three layers constitute the front-contact, the solar-absorber and the back-contact layers.

In order to generate required voltage, solar cell panels are structured by scribing parallel lines in various thin film layers. This scribing of the thin films is where DPSS q-switched lasers are most widely applied. Typically, the following three scribe processes are performed during cell manufacturing: P1 scribe, which removes a conducting layer from the glass substrate; P2 scribe, which removes semiconductor layer from the material scribed in the P1 process; and P3 scribe, which removes all of the final electrical contact layer and some or all of the solar-absorber (P2-scribe) material. The three scribe lines are arranged parallel to one another and as closely as possible on the large flat panel.

## Laser Beam Shape Comparison

While DPSS laser processing has achieved great success with a variety of TFPV scribe processes, there are potentially some areas for improvement. For example, depending on the thin film material property or deposition technique, sometimes cracks or lifting of the material can occur at the scribe edges. To improve

the quality of scribes and to increase throughput of the process, advantages of using flattop beam shape instead of fundamental Gaussian beam shape have been discussed in the literatures [2].

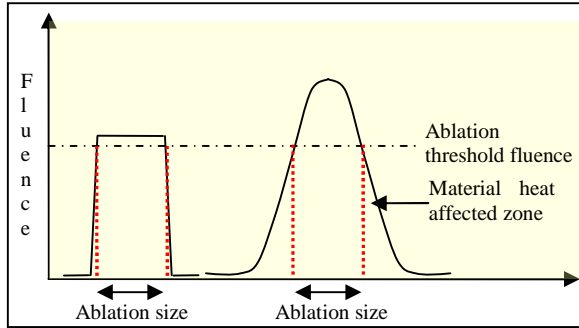


Figure 1: Gaussian and flattop beam intensity distribution

Figure 1 illustrates the differences between Gaussian and flattop beam fluence distributions as they relate to thin film ablation. For the Gaussian beam, there is a tendency for strong ablation at the center of the beam where the intensity can be significantly higher than the ablation threshold. This can potentially result in unwanted damage to the underlying layers of the material. Furthermore, if the fluence at the edges of the Gaussian is just below the ablation threshold of the material, it can lead to heating of the material and bad quality of scribes. Outside of the proper processing window (assuming one exists), both of these effects can lead to unwanted material modification such as micro-cracks, film delamination, etc.

One of the ways to eliminate or reduce such ill effects is to use a “flattop” beam for scribing. In recent years, variety of products is available in the markets that are designed to efficiently convert a Gaussian laser beam to a flattop beam. Thus for a flattop uniform beam distribution, once it is above the ablation threshold the same amount of material will be removed across the entire defined flattop region. Thus the center of the ablation area will be less likely to cause unwanted collateral damage to underlying material(s). In addition, the sharp drop in fluence at the edge of the beam implies the potential for minimal heat affected zone at the edges of the laser-processed region. While there are clearly benefits in using flattop beam for scribing, it is unclear if there are any negative effects of using flattop beam over Gaussian beam.

To explore this further, in this paper scribes generated with Gaussian and flattop beams have been characterized in terms of scribe quality and their electrical isolation measurements. Quality

considerations include damage to underlying substrate material and lifting/peeling/cracking of the film(s) at the scribe edges. Furthermore, the processing depth of focus for the two beam shapes is characterized by defocusing the optical system in small steps and quantifying the resulting change in electrical isolation of the scribes. For this study, the material chosen was Molybdenum thin film on glass. The film thickness is ~300nm, and the glass thickness is ~1 mm. Molybdenum thin film is used as a rear contact electrode in CIGS (Copper Indium Gallium Diselenide) solar cells. Lasers are used to scribe lines on Molybdenum thin film for electrical isolation as an early step in manufacturing of these cells.

### Laser Beam Quality Comparison

We have also studied the effect of TFPV scribing using a high- vs. low-quality Gaussian laser beams. For every Gaussian laser beam, there exists the beam propagation (“quality”) value, known as the  $M^2$  factor. A laser beam with  $M^2$  factor of 1 is considered a diffraction limited ideal laser beam; an  $M^2$  factor very close to 1 is considered a good quality beam.

From a system design perspective, the effect of the  $M^2$  factor could be significant. For example, a high- $M^2$  beam will diverge more rapidly than a low- $M^2$  beam when focused to the same optical spot size. Because of the resultant larger spot size which results in lower fluence, this increased divergence would then be expected to reduce the processing depth of focus for a particular scribe process. Figure 2, which compares high- and low- $M^2$  Gaussian beam focusing, illustrates this potential problem.

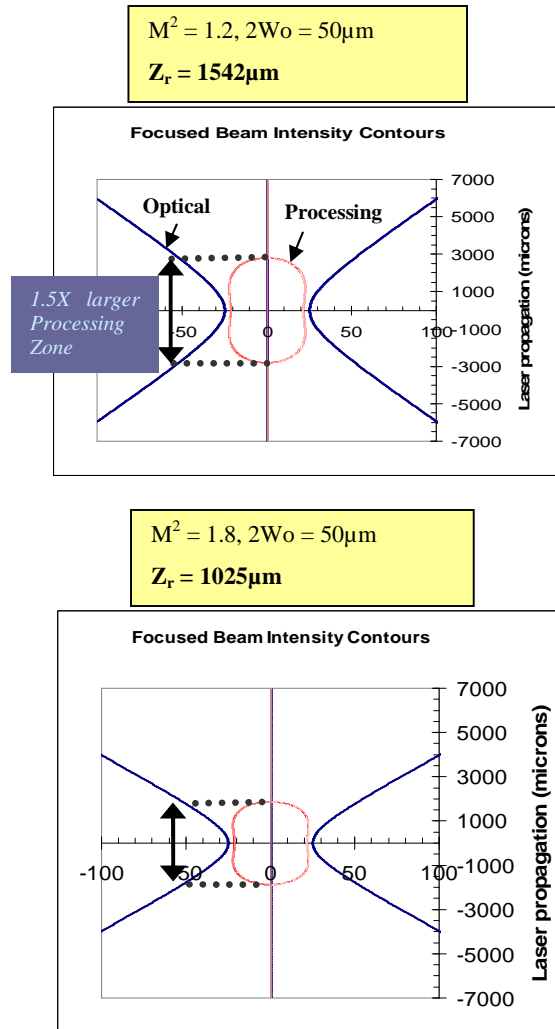


Figure 2: Theoretical depth of focus (DOF) variation between different  $M^2$  value lasers.

In Figure 2, the incident focused laser beam is viewed from a side-view perspective, with the horizontal axis representing the surface of the target material, and the vertical axis representing the beam propagation direction (i.e. optical Z-axis).  $M^2$  of 1.8 versus 1.2 implies  $(1.8/1.2=)$  1.5X system defocus tolerance advantage for a laser with smaller  $M^2$  value.

To characterize the effect of beam quality ( $M^2$  value) on the process depth of focus, scribe de-focusing tests similar to one described above in the Gaussian vs. flattop tests were performed. Electrical isolation scribes were generated with varying degrees of system defocusing with both high- and low- $M^2$  laser beams. The quality and electrical isolation capability of these scribes was then characterized. The material of study for this experiment is thin film tin oxide ( $\text{SnO}_2$ ) coated on glass. The thickness of the film is  $\sim 600\text{nm}$ , and the

glass substrate thickness is  $\sim 3.8\text{mm}$ .  $\text{SnO}_2$  is commonly used as a transparent front electrode in a-Si (amorphous silicon) and CdTe (Cadmium Telluride) solar cells.

## Experiment Details

### Laser System

Laser Beam Shape Comparison Gaussian and flattop shaped laser beam experiments were performed using Newport-Spectra Physics DPSS q-switched Pulseo<sup>®</sup> 532nm laser. Detailed laser specifications are mentioned in Table 1.

Table 1: Specifications of laser system used for laser beam shape comparison experiments.

Parameters	Pulseo <sup>®</sup> laser
Wavelength	532 nm
Peak Power	>34 W at 120kHz
Repetition Range	1 Hz-300 kHz
Pulse Width	<30ns
$M^2$	<1.3
Beam Diameter	3.5mm

Laser Beam Quality Comparison Experiments to study beam quality were performed using different  $M^2$  value infrared (IR) lasers. Detailed laser specifications are mentioned in Table 2.

Table 2: Specifications of laser systems used for laser beam quality comparison experiments.

Lasers	HIPPO	Prototype
Laser Type	DPSS q-switched	Fiber (pulsed)
Power	17W at 50 kHz	20W
Repetition Range	15-300 kHz	20-200 kHz
Pulse Width	<15 ns	15ns
$M^2$	<1.2	1.8

### Optical Setup

Laser Beam Shape Comparison The Gaussian beam machining setup consisted of the Pulseo<sup>®</sup> laser system with 3.5mm diameter output beam routed via 4 steering mirrors into a galvanometer scanner ( $\Phi=14\text{mm}$ ) and 254mm f-theta lens to achieve  $\sim 140\mu\text{m}$  ( $1/e^2$ ) focus spot size.

The flattop beam machining setup consisted of the Pulseo<sup>®</sup> laser system with 3.5mm diameter output beam optically reduced to 2mm size at the diffractive optical element (DOE). The beam was steered by 4 steering mirrors into a galvanometer scanner

( $\Phi=14\text{mm}$ ) with an 80mm focal length f-theta lens to create  $\sim 68\mu\text{m}$  flattop intensity distribution at the image plane. A schematic illustration of the optical setup is shown in Figure 3. The DOE converts the 2mm Gaussian beam into a  $1.63\text{mm}\times 1.63\text{mm}$  square flattop beam. This  $1.63\text{mm}$  square beam is used as an object which is imaged onto the target material using the 80mm focal length f-theta lens. This lens, located  $\sim 1.9$  meters from the object plane, produces a  $\sim 68\mu\text{m}$  sized flattop image on the work piece. The optical efficiency of the setup was found out to be  $\sim 71\%$  including losses by lens, DOE, mirrors, scanner and f-theta lens. The efficiency obtained is somewhat low due to some beam clipping which occurred at the 14-mm galvanometer aperture. Although the clipping is undesirable, this setup was found to be optimal for generating a small ( $68\mu\text{m}$  diameter) flattop with the available equipment. Increased optical efficiency while maintaining a similarly-small flattop beam size could be achieved with, for example, a larger-diameter scan head aperture.

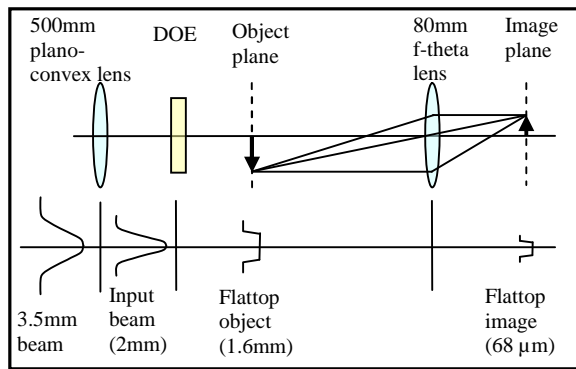


Figure 3: Schematic illustration of flattop experimental optical setup and intensity distribution

**Laser Beam Quality Comparison** The experimental setup using high beam quality laser (low  $M^2$  value) consisted of HIPPO DPSS q-switched laser system ( $M^2 < 1.2$ ) with a beam steered by 4 steering mirrors into a galvanometer scanner ( $\Phi=14\text{mm}$ ) and 163mm f-theta lens to create  $\sim 50\mu\text{m}$  ( $1/e^2$ ) focus spot size.

The setup to study the effect of low beam quality consisted of a prototype fiber laser ( $M^2=1.8$ ) with a beam steered by 4 steering mirrors into a galvanometer scanner ( $\Phi=14\text{mm}$ ) with 80mm focal length f-theta lens to create  $\sim 50\mu\text{m}$  ( $1/e^2$ ) focus spot size.

## Results and Discussion

### Laser Beam Shape Comparison

**Gaussian Beam Machining** Gaussian beam scribing of the Molybdenum thin film material was performed

with the laser incident on the film side of the sample. Optimal conditions for laser scribing were found to be  $6\text{m/s}$  scan speed with  $\sim 18\%$  pulse overlap at  $100\text{kHz}$  repetition rate. Using  $\sim 3\text{W}$  on-target power at  $100\text{kHz}$  resulted in  $\sim 70\mu\text{m}$  wide scribes with minimal damage to underlying substrate.

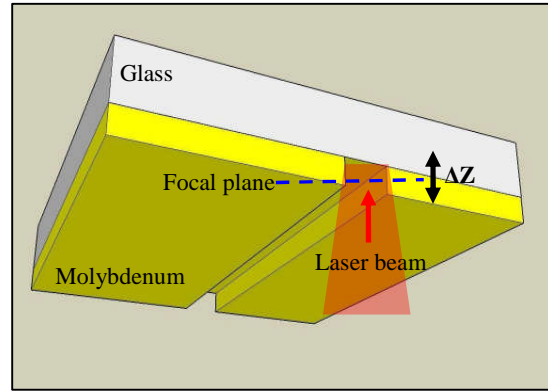


Figure 4: Gaussian beam shape laser machining

For the defocusing test, electrical isolation test scribes were machined at the focal plane and at defocus positions of  $\pm 20\text{mm}$ , with  $4\text{mm}$  step size. For reference, Figure 4 contains a schematic illustration of the defocusing setup and procedure.

Good quality scribes were obtained by machining scribes at the focal plane. Figure 5 shows an optical microscope photo and a 3-dimensional depth profile of a scribe at the focal plane. 3D depth profile data was obtained using mechanical stylus profilometer which was programmed to execute multiple adjacent steps and repeat scans, resulting in the generation of 3-dimensional topographical data. 3D profile shows complete Molybdenum film removal without damage to the glass substrate.

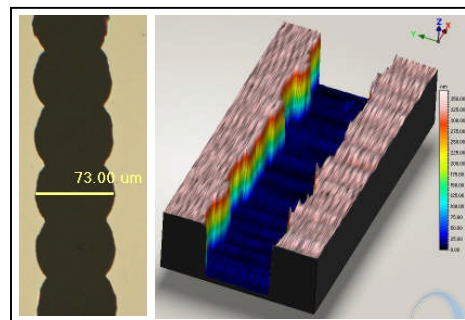


Figure 5: Gaussian machining microscope picture and 3D depth profile of a scribe at the focal position (Power= $3\text{W}$ ;  $100\text{kHz}$  at  $6\text{m/s}$  scan speed)

Figure 6 shows scribes at different defocus positions going away from the focal plane. The quality of the scribes is observed to be maintained with clean Molybdenum film removal for a distance of +/-17mm around the focal plane. There is no significant change in the scribe width within +/-17mm distance from the focal plane. Going beyond +/-17mm defocus position, flaking at the edges of the scribes is observed, leading to reduced quality and irregular scribe width. Ablation of the material ceases altogether beyond +/-24mm defocus distance.

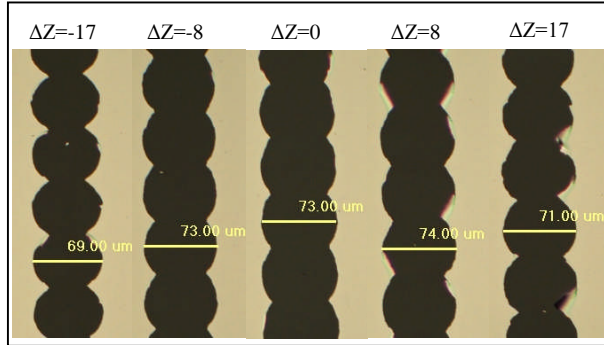


Figure 6: Microscope pictures of Gaussian beam scribes at different defocus positions ( $\Delta Z$ ) w.r.t focal position

Flattop Beam Machining 68 $\mu$ m flattop beam with uniform intensity distribution was used to scribe lines in the Molybdenum sample at 5.6m/s scan speed at 100 kHz pulse repetition rate to maintain ~18% pulse overlap similar to Gaussian beam machining experiment. The laser incidence was on the film side of the sample, as depicted in Figure 7.

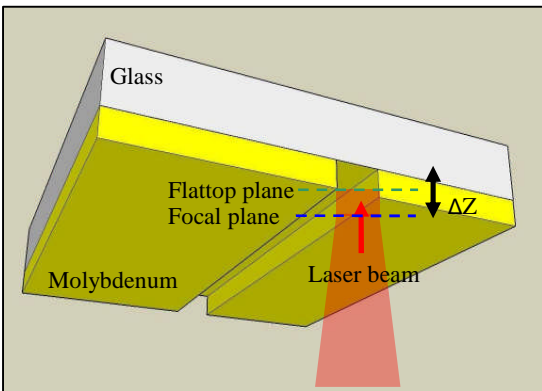


Figure 7: Flattop beam shape laser machining

2.1W on-target power at 100kHz was found to be optimal condition for complete Molybdenum film removal without damage to the glass substrate.

Electrically isolating scribes were processed on Molybdenum sample using flattop beam shape.

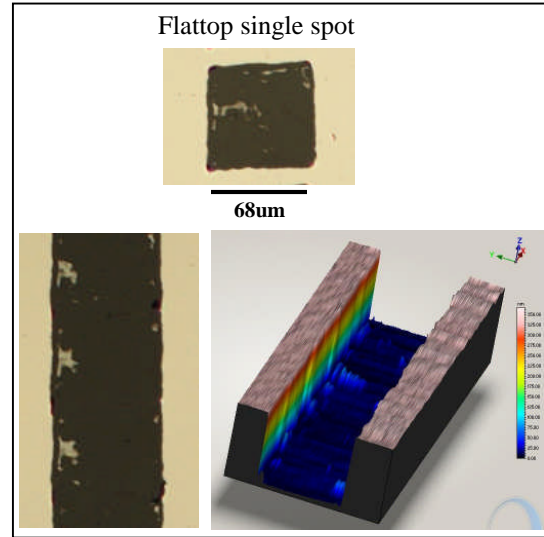


Figure 8: Flattop machining microscope picture of a single spot, scribe and 3D depth profile of a scribe at the focal position (Power=2.1W; 100kHz at 5.6m/s scan speed)

Figure 8 shows a microscope picture of a single spot ablation and a scribe processed at the focal plane. Quality of scribe at the flattop plane is good with smooth edges. Due to slight variation in the intensity distribution along the flattop plane, some residual material is observed to be left behind.

Defocusing test was performed by machining scribes at different defocus positions ( $\Delta Z$ ) going 1.6mm distance away from the flattop image plane in each direction. Beam was moved along Z direction in steps of +/-0.1mm  $\Delta Z$  distance. Scribes for electrical isolation were generated at each position to measure resistance of the scribes. Figure 9 shows microscope pictures of the scribes at different defocus positions from the flattop plane. Shape and size of the flattop beam dramatically changes even within 1mm distance from the flattop plane. More and more residual material is seen to be left behind going away from the flattop image plane in Z direction.

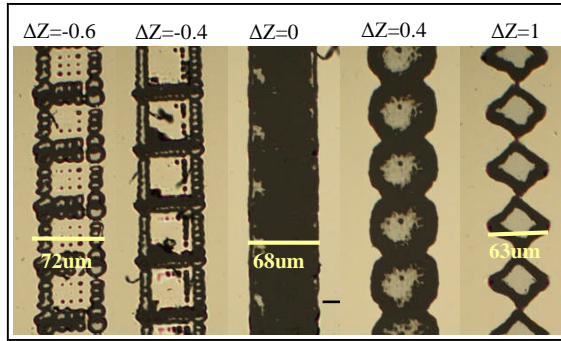


Figure 9: Microscope pictures of flattop beam scribes at different defocus positions ( $\Delta Z$ ) w.r.t flattop plane

**Resistance Measurements** Electrical resistance of isolating scribes machined at various defocus positions using Gaussian and flattop shaped laser beams were measured and compared as shown in Figure 10.

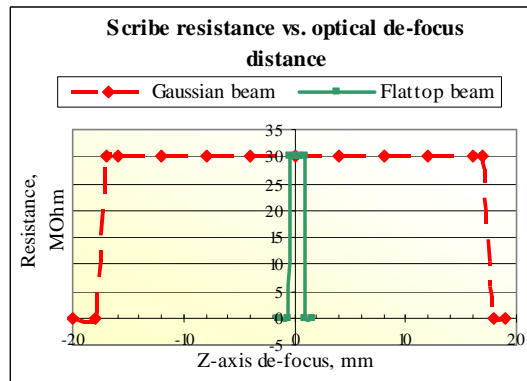


Figure 10: Electrical resistance measurement of scribes processed at various defocus positions

30Mohm is the measurement limit of the instrument used to measure the resistance of scribes. 30Mohm measured electrical resistance suggests that film is completely removed without any material residue left behind to conduct current across the scribe. For Gaussian beam machining, electrically isolating scribes are obtained within  $\pm 17$ mm distance on either side of the focal plane. Also, the shape and size of the scribes do not change significantly within the  $\pm 17$ mm defocus range. Resistance is observed to decrease for scribes machined beyond  $\pm 17$ mm from the focal plane. This implies that for  $\sim 70\mu\text{m}$  scribe width at the focal plane, Gaussian beam machining has about  $\pm 17$ mm defocus tolerance. This is of great advantage from a system design perspective, since positioning tolerances on the order of 10's of mm should not be difficult or costly to achieve.

For flattop beam machining, it is observed that electrically isolating scribes are obtained within  $-0.5$ mm and  $1$ mm ( $\Delta Z$ ) distance from the flattop plane. So from system design perspective, total depth of focus tolerance for a  $68\mu\text{m}$  flattop beam machining is only  $1.5$ mm. Also, it is observed that the shape of the scribes dramatically changes within  $1.5$ mm distance as seen from Figure 9. Within  $<0.5$ mm defocus distance, the flattop beam distribution completely collapses, resulting in what appears to be significant variations in energy density ("hot spots"). Thus, while the defocus tolerance for measurable electrical isolation is found to be  $\sim 1.5$ mm, it is clear that the tolerance for clean, uniform flattop beam machining is considerably less than  $0.5$ mm.

These results demonstrate that for making  $\sim 70\mu\text{m}$  wide scribes, flattop beam processing allows  $\pm 1$ mm (at most) defocus tolerance compared to  $\pm 17$ mm for a Gaussian beam. Clearly, Gaussian beam machining has a significant advantage in accommodating 1 to 3mm glass flatness and other variations associated with large solar panels and can provide a wide robust processing window.

### Laser Beam Quality Comparison

**High Beam Quality Machining Scribes on  $\text{SnO}_2$**  sample were machined using DPSS q-switched IR HIPPO laser ( $M^2 < 1.2$ ) with  $\sim 50\mu\text{m}$  ( $1/e^2$ ) optical spot size. The laser incidence was from the glass side of the sample. Optimal settings for the clean ablation scribes were found to be 17W at 100 kHz with 3m/s scribe speed. Figure 11 contains a schematic illustration of the defocusing setup and procedure.

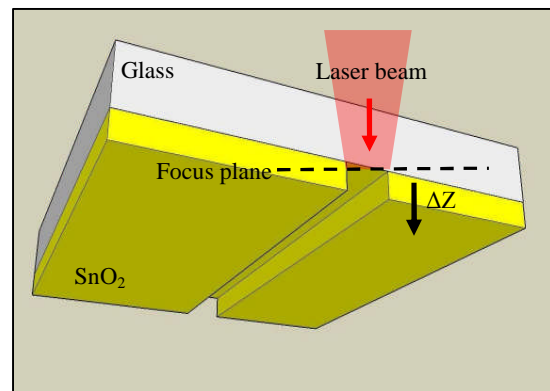


Figure 11: Laser beam quality experiment machining

Defocusing test was performed by machining scribes at different focal positions going  $3.3$ mm distance away from the focal plane in one direction. Beam was defocused in steps ( $\Delta Z$ ) of  $0.3$ mm distance. Electrically isolating scribe pattern was generated to

measure resistance of the scribes at different focal positions. Figure 12 shows microscope pictures of the scribes at different defocus positions.

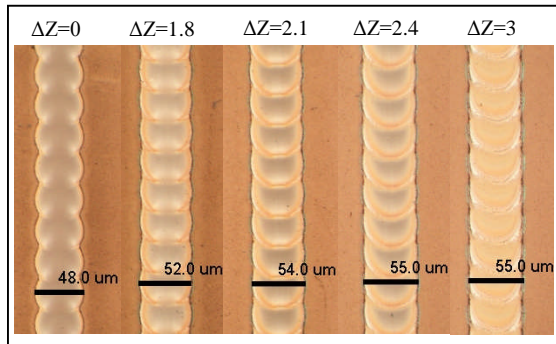


Figure 12: Microscope pictures of DPSS q-switched laser ( $M^2 < 1.2$ ) machining on  $\text{SnO}_2$  sample at various defocus positions (Power=17W; 100kHz at 3m/s scan speed)

From Figure 12, it is seen that the quality of scribes is maintained with clean  $\text{SnO}_2$  film removal along 2.4mm defocus distance. Going beyond 2.4mm defocus position, quality of scribes degrades with decrease in scribe width.

**Low Beam Quality Machining** Scribes on  $\text{SnO}_2$  sample using fiber laser with  $M^2=1.8$  were machined using IR fiber laser with  $\sim 50\mu\text{m}$  ( $1/e^2$ ) optical spot size. The laser incidence was on glass side of the sample. Optimal settings for clean ablation scribes were found to be 16.5W at 125 kHz with 3m/s scribe speed.

Defocusing test was performed by machining scribes at the focal plane and going 2mm distance away from the focal plane in one direction. Beam was defocused in steps of 0.4mm distance. Electrically isolating scribe pattern was generated to measure resistance of the scribes at different defocus positions. Figure 13 shows microscope pictures of the scribes at different defocus positions.

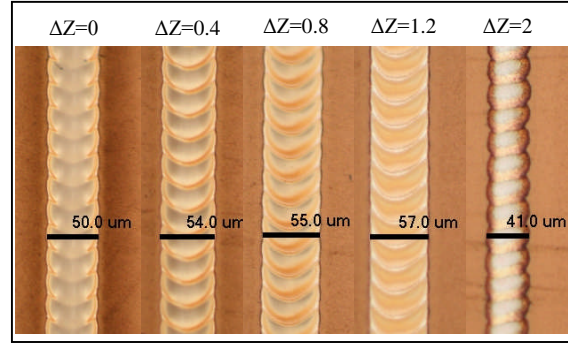


Figure 13: Microscope pictures of fiber laser ( $M^2=1.8$ ) machining on  $\text{SnO}_2$  sample at the focal plane and away from the focal plane (Power=16.5W; 125 kHz at 3m/s scan speed)

Quality of scribes is observed to be good only within 1.2mm defocus distance. Scribe width is seen to be increasing within 1.2mm distance from the focal plane and then starts decreasing going further.

To explain the change in scribe width phenomenon, Figure 14 demonstrates change in intensity of Gaussian beam (which affects scribe width) going away from the focal plane. Going away from the focal plane as the spot size increases, peak fluence of the Gaussian profile starts to decrease and at some point comes close to ablation threshold of the material. Material is seen to be removed only at the portions where fluence is above ablation threshold which is at the center of the Gaussian. Change in scribe width phenomenon is particularly observed when peak fluence at the focal plane is well above ablation threshold fluence of material.

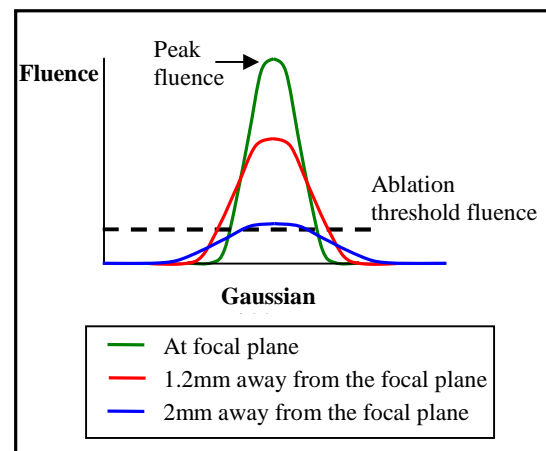


Figure 14: Change in intensity of Gaussian beam going away from the focal plane

**Resistance Measurements** Electrical resistance of isolating scribes machined at various defocus positions using different beam quality lasers were measured and compared as shown in Figure 15.

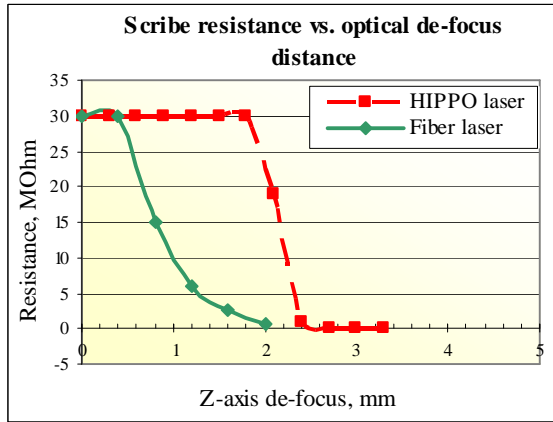


Figure 15: Electrical resistance measurement of scribes processed at various defocus positions

Again, 30Mohm measured electrical resistance suggests that film is completely removed without any material residue left behind to conduct current across the scribe. DPSS Q-switched laser with  $M^2 < 1.2$  showed good electrical isolation resistance of 30Mohm within 2.1mm distance from the focal position. Resistance is observed to decrease for scribes machined beyond 2.1mm distance. For a pulsed fiber laser with  $M^2 = 1.8$  electrically isolating scribes were achieved within 0.4mm distance away from the focal plane. Electrical resistance drops to a low value for scribes machined beyond 0.4mm. This indicates that for an optical system, defocusing tolerance for high quality q-switched laser Gaussian beam is  $\sim \pm 2$ mm whereas for a pulsed fiber laser with comparatively low quality beam the system defocus tolerance is  $\pm 0.4$ mm. This suggests that for a low beam quality laser system there is very narrow de-focus scribe tolerance range and it cannot accommodate 1 to 3mm glass flatness and other variations associated with large solar panels and it cannot provide a wide robust processing window.

### Conclusions

Two different experiments were conducted to characterize effect of laser beam shape (Gaussian Vs flattop) and laser beam quality (high Vs low  $M^2$ ) on process depth of focus. Electrically isolating scribes were machined in Molybdenum and  $\text{SnO}_2$  thin films deposited on a glass substrate at various defocus positions. Scribes quality and electrical resistance were

characterized to determine acceptable process depth of focus.

In the laser beam shape comparison experiment, for  $\sim 70\mu\text{m}$  wide scribes in Molybdenum, defocus tolerance for Gaussian beam machining was found to be  $\pm 17$ mm whereas for  $68\mu\text{m}$  wide scribes in  $\text{SnO}_2$  defocus tolerance for flattop beam machining was found to be  $< \pm 1$ mm. Good quality scribes were obtained within  $\pm 17$ mm defocus range for Gaussian beam and  $< 0.5$ mm defocus range for flattop beam machining.

In the laser beam quality comparison experiment, scribes were machined using high beam quality DPSS q-switched laser with  $M^2 < 1.2$  and low beam quality prototype pulsed fiber laser with  $M^2 = 1.8$  at various defocus positions on  $\text{SnO}_2$  thin film. In case of high beam quality machining, electrically isolated good quality scribes were obtained within  $\sim \pm 2.0$ mm defocus range while for low beam quality machining good quality scribes were obtained only within  $\pm 0.4$ mm defocus range.

While both flattop laser beam shape and low beam quality laser can produce a good quality scribes, in both cases a very small process depth of focus tolerance range exists. This is undesirable from system design perspective since systems are required to accommodate up to 1 to 3mm variations associated with processing of large solar panel glass thickness variation and other system tolerances. Whereas, once acceptable process parameters are defined for a low  $M^2$  Gaussian DPSS nanosecond laser beam scribing process, such system is capable of accommodating large process defocus variation and it provides a wide robust processing window for a high yield low cost laser scribing manufacturing process.

### References

- [1] Patel, R., Clark, D. & Bovatsek, J. (2007) Laser scribing: A key enabling technology for manufacturing of low cost thin film photovoltaic cells, in Proceedings of ICALEO Conference in Orlando, Florida, 113-118.
- [2] Homburg, O., Volkermeier, F., Toennissen, F., Ganser, H. & Mitra, T. (2007) High-precision Gaussian-to-tophat beam transformation improves structure quality and speed in micro-machining, in Proceedings of WLT Conference on Lasers in Manufacturing, Munich, Germany.

## Meet the Authors

Ashwini Tamhankar is a senior laser applications engineer at Newport Corporation's Spectra-Physics Lasers division in Mountain View, California. She has been working in the lasers and optics industry since 2004, where she has gained broad experience in areas such as laser technology development, optical system design, laser beam shaping techniques and laser application development with nanosecond pulsed lasers. She has earned her M.S. Physics degree from San Jose State University in 2005 and M.Sc. Solid State Physics degree from Shivaji University (India).

Jim Bovatsek is a senior laser applications engineer at Newport Corporation's Spectra-Physics Lasers division in Mountain View, California. He has focused on laser application development with nanosecond, picosecond, and femtosecond pulsed lasers since 2000. He received his Bachelors in Science, Physics degree from the University of California, Santa Barbara in 1997.

Gonzalo Guadano is currently working at Lasing S.A; a Technical company in Spain specialized in photonics and automation. In 2008 he worked as a temp. at Newport Corporation's Spectra-Physics Lasers division in Mountain View, California where he gained experience in laser micromachining using DPSS q-switched nanosecond and fiber lasers. He also worked at The Laser Center of Madrid in 2007. He earned his Master's degree in Photonics from Autonoma University, Madrid in 2008 and a degree in Industrial Engineering specializing in Automation and Electronic from Polytechnic University, Madrid in 2006.

Rajesh (Raj) S. Patel has accumulated 21 years of experience in the laser material processing field. He is currently a manager at Spectra Physics, a division of Newport Corporation, and is responsible for managing laser processing applications lab. Prior to working at Spectra Physics he has also worked at IBM, Aradigm, and IMRA America in the past. He received his Ph.D. degree in mechanical engineering from the University of Illinois at Urbana-Champaign in 1989. His professional interests are in the areas of laser development, laser material processing and equipment design, mask technology, optics, and application of lasers in various fields. He has worked with various lasers for developing applications in microelectronics, semi-conductor, bio-medical, and the photonic industry. He is an author of 22 U.S. patents related to laser processing, optics, and the mask technology field and has published and presented more than 45 technical papers.